INSTITUTE OF PHYSICS PUBLISHING JOURNAL OF OPTICS A: PURE AND APPLIED OPTICS

J. Opt. A: Pure Appl. Opt. **4** (2002) S207–S211 PII: S1464-4258(02)53449-8

Optical properties of cross-conjugated isopolydiacetylene oligomers as measured by ultraviolet–visible spectroscopy and the optical Kerr effect

Aaron D Slepkov[1], Frank A Hegmann[1], Kenji Kamada[2], Yuming Zhao[3] and Rik R Tykwinski[3]

[1] Department of Physics, University of Alberta, Edmonton, Alberta, Canada T6G 2J1
[2] Photonics Research Institute, National Institute of Advanced Industrial Science and Technology (AIST), Ikeda, Osaka 563-8577, Japan
[3] Department of Chemistry, University of Alberta, Edmonton, Alberta, Canada T6G 2G2

E-mail: hegmann@Phys.ualberta.ca, k.kamada@aist.go.jp and rik.tykwinski@ualberta.ca

Received 31 January 2002
Published 30 October 2002
Online at stacks.iop.org/JOptA/4/S207

Abstract
A novel series of isopolydiacetylene oligomers have been characterized on the basis of their electronic absorption, emission and nonlinear optical properties. The ultraviolet–visible spectra indicate only a small shift to lower energy as a function of increasing oligomer length. To evaluate the third-order nonlinear susceptibilities, $\chi^{(3)}$, and second hyperpolarizabilities, γ, of these oligomeric samples a new Kerr gate technique, differential optical Kerr effect detection, has been employed. A linear relationship between γ and the number of repeat units is found, suggesting that the fixed-length linearly conjugated segments dominate the electronic polarizability. The largest nonlinearity was observed in the heptamer sample, displaying a second hyperpolarizability relative to the tetrahydrofuran solvent of $\gamma_{heptamer}/\gamma_{THF} = 181 \pm 9$.

Keywords: Nonlinear optics, optical Kerr effect, conjugated oligomers, polydiacetylenes, alkynes

1. Introduction

The delocalized electronic structure of π-conjugated organic compounds offers a number of tantalizing opportunities for applications as nonlinear optical (NLO) materials. For practical applications, organic nonlinear materials will also require transparency, stability, rapid response times and processability [1–3]. The ease with which one can systematically vary the framework of organic molecules provides a remarkable opportunity to probe the relationship between structure and function, and these analyses have become the foundation of any effort toward the optimization of optical materials [4–7].

Studies of linearly conjugated polydiacetylenes (figure 1) have shown these materials to have significant third-order nonlinearities [8]. Both experimentally and theoretically it is clear that extending the π-conjugated path of polydiacetylenes significantly enhances the observed nonlinearities [2, 6, 9, 10]. As the conjugation length increases, however, the wavelength of the lowest-energy absorption maximum, λ_{max}, increases as well. This ultimately yields materials with insufficient transparency for many applications [11–13]. It is clear that attempts to maximize $\chi^{(3)}$ by simply increasing the length of the linearly conjugated backbones are unlikely to produce practical NLO materials [4].

In an attempt to identify molecular designs that could provide both conjugated and transparent materials, we targeted cross-conjugated oligomeric compounds. Because π-delocalization is less efficient across a cross-conjugated bridge than in an analogous linearly conjugated arrangement, we were intrigued as to the possibility of increasing the optical nonlinearities, while at the same time preserving the electronic transparency.

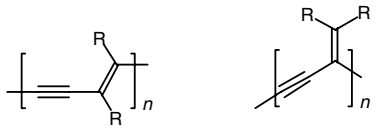

Figure 1. Repeat unit building blocks for polydiacetylene (PDA) and isopolydiacetylene (iso-PDA) oligomers.

A series of monodisperse cross-conjugated iso-PDA oligomers (iso-PDAs) has been synthesized with phenyl substituents. The third-order NLO characteristics were measured using a new technique, the differential optical Kerr effect (DOKE) detection setup shown in figure 2 [14]. This detection method is similar to various optical biasing schemes routinely used in the field of free-space electro-optic sampling of terahertz pulses [15, 16].

2. Experimental considerations

The optical Kerr effect (OKE) is an optically induced birefringence in an isotropic medium [17]. In a standard Kerr gate [18–20], an intense, linearly polarized pulse induces a birefringence in an isotropic medium. The anisotropy in the sample's index of refraction ($\delta n = \delta n_{\parallel} - \delta n_{\perp}$, the difference in refractive index between parallel and perpendicular axes to the pump polarization) induced by the pump pulse is then probed by a second, weaker, pulse. The induced birefringence, δn, manifests itself as retardation in the probe beam polarization and may be detected using a polarizer acting as an analyser. A temporal profile of the induced birefringence may be obtained by time-delaying the arrival of the probe pulse. When the pump and probe pulses arrive simultaneously at a sample dominated by an ultrafast electronic nonlinearity, the probe beam experiences the maximum rotation in polarization given by

$$\phi = \frac{2\pi d}{\lambda} n_2 I_{pump}, \tag{1}$$

where n_2 is the nonlinear index of refraction and is proportional to $\chi^{(3)}$, λ is the wavelength, d is the sample length and I_{pump} is the pump intensity in units of W m^{-2}. The quantity n_2 is a modification to the linear index of refraction where the total index of refraction is given by $n = n_0 + n_2 I_{pump}$, with n_0 being the linear index of refraction. $\chi^{(3)}$ is obtained from n_2 by [21]

$$n_2\left(\frac{m^2}{W}\right) = \frac{3.9 \times 10^{-6}}{n_0^2}\chi^{(3)}\,(\text{esu}), \tag{2}$$

where n_2 is in units of m^2 W^{-1} and $\chi^{(3)}$ is in esu [21]. The molecular second hyperpolarizability, γ, may be obtained by [3]

$$\gamma = \frac{\chi^{(3)}}{N_c L^4}, \tag{3}$$

where N_c is the molecular number density in cm^{-3} and L^4 is the Lorentz field-factor which, for isotropic liquid media is approximated by $[(n_0^2 + 2)/3]^4$.

To separate the real and imaginary components of $\chi^{(3)}$ and to obtain larger signals, optical heterodyne detection–optical Kerr effect (OHD–OKE) is used by many groups [22, 23]. In OHD–OKE, a quarter-wave plate ($\lambda/4$) is placed between the probe polarizer and sample such that the fast axis of the quarter-wave plate is parallel to the polarizer. By slightly rotating the polarizer, $\pi/2$ out-of-phase light is added to the probe beam, and this technique can provide the real or imaginary components of the nonlinear response directly from the Kerr signal. In this arrangement, for small responses, transmitted signals are linear with pump intensities.

The DOKE setup shown in figure 2 uses pump and probe pulses generated by an amplified Ti:sapphire laser, producing 800 nm, <100 fs pulses at a 1 kHz repetition rate. A computer-controlled retroreflector is used to vary the delay between the pump and probe pulses. The pump pulse is polarized 45° to the horizontal before being focused onto a 1.0 mm sample-path-length quartz cuvette filled with a sample solution. The weaker probe beam is initially polarized vertically and then passes through a quarter-wave plate oriented to produce circular polarized light. Typical pump and probe powers at the sample location are between 0.5 and 6 mW for the pump beam and 50 and 80 μW for the probe beam. The probe light is focused to overlap in the sample with the pump beam at a near coincident angle, $\theta < 5°$. Typical spot sizes for the pump and probe beams are ~500 and 240 μm respectively. After passing through the sample, the pump beam is blocked while the probe beam is allowed to travel to a Glan-laser polarizer acting as the analyser. Here, the transmitted and rejected beams are directed to a pair of balanced photodiodes where photodiode 'A' receives the rejected beam and photodiode 'B' receives the transmitted beam. The pump beam is chopped at 125 Hz, and lock-in detection is used to monitor the A − B signal. The A + B signal is detected at 1 kHz using a separate lock-in amplifier. Finally, these signals are sent to a computer used for data acquisition and delay-stage control.

The key feature of the DOKE setup is that A − B acts as the Kerr effect signal detection and, if $\text{Im}(\chi^{(3)})$ is small, A + B acts as a probe beam reference. In the presence of nonlinear absorption, such as two-photon absorption, the A + B signal provides independent detection of $\text{Im}(\chi^{(3)})$ processes. The photodiodes are calibrated such that in the absence of any birefringence, A and B signals are equal and A − B is zero.

Consider a vertically polarized probe beam and a sample with an induced birefringence of $\phi = \phi' + \text{i}\phi''$, where ϕ' and ϕ'' are the real and imaginary components of the phase retardation, respectively. If after passing through a quarter-wave plate set with fast axis at 45° the beam is incident on the sample, the detected signal ratio is given by

$$\frac{A - B}{A + B} = \frac{\sin\phi'}{\cosh\phi''}. \tag{4}$$

This relationship is valid when the pump and probe beams are initially polarized at 45° with respect to each other. In the absence of nonlinear absorption, $\phi'' = 0$, and equation (4) is reduced to equation (5), a purely real response:

$$\frac{A - B}{A + B} = \sin\phi'. \tag{5}$$

Much like the heterodyne scheme, DOKE detection obtains signals that are linear with pump and probe intensity. The DOKE technique affords a larger dynamic range of linear

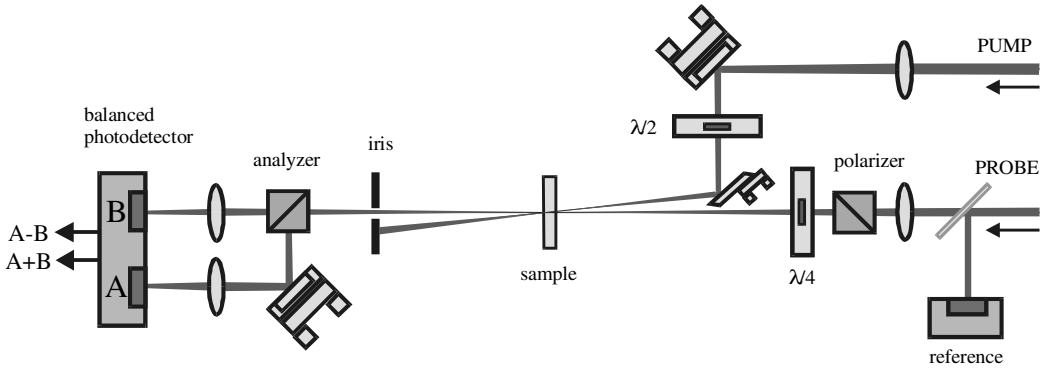

Figure 2. Schematic outline of the DOKE detection setup.

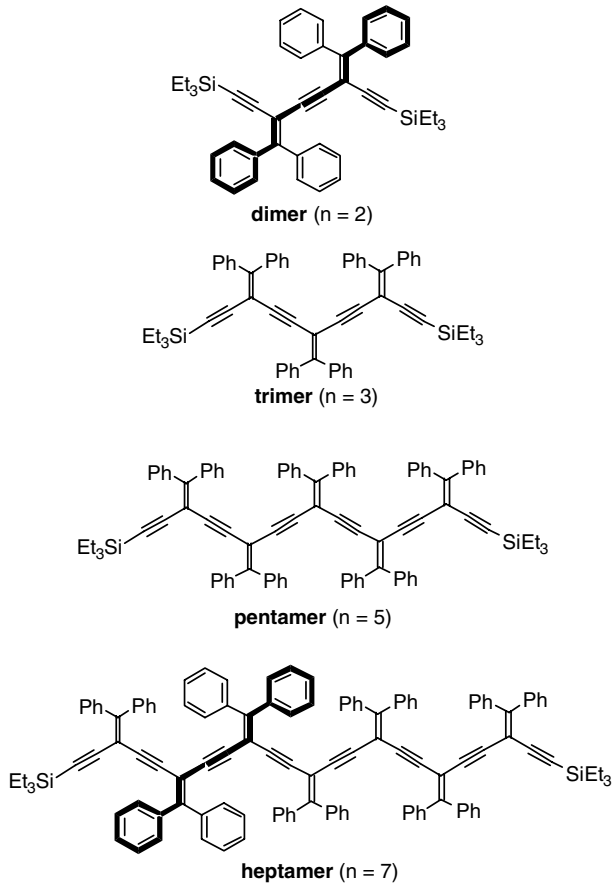

Figure 3. Iso-PDA oligomers investigated in the current study. The bold lines highlight the longest linearly conjugated path in the dimer and heptamer.

signal than the typical heterodyne scheme. We have also observed that the DOKE signals are larger than those obtained with OHD–OKE, making detection easier. A full description of the DOKE technique will be presented elsewhere.

The iso-PDA oligomers used in this study are shown in figure 3. (Details of their synthesis will be published elsewhere [24].) NLO samples were prepared by dissolving the oligomer sample in high-purity tetrahydrofuran (THF) to give solutions of 0.1–0.23 M. All samples were measured within 24 h of preparation.

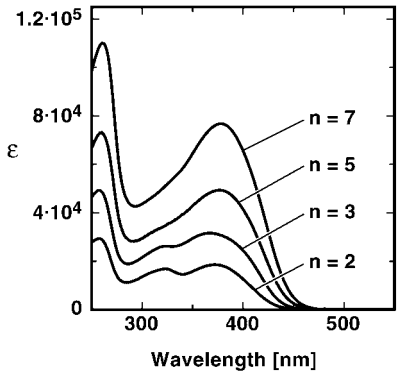

Figure 4. Electronic absorption spectra for iso-PDAs, as measured in $CHCl_3$.

Table 1. Linear and NLO data for iso-PDAs.

n	λ_{max} (nm) (ε, 1 M^{-1} cm^{-1})	$\lambda_{emission}$ (nm)	γ_S ($\times 10^{-36}$ esu)	γ_S/γ_{THF}
2	373 (18 500)	475	30.3 ± 0.3	58 ± 0.5
3	367 (31 600)	489	49 ± 4	94 ± 7
5	377 (49 300)	498	69 ± 5	134 ± 9
7	378 (76 800)	501	95 ± 4	181 ± 9

3. Results and discussion

The electronic absorption data for the iso-PDA dimer through the heptamer are shown in figure 4, and the lowest-energy absorption maxima (λ_{max}) are listed in table 1. There is a slight shift in λ_{max} values as the chain length is extended from the dimer through the heptamer. By the stage of the heptamer, this effect appears to have reached saturation at 378 nm, and longer oligomers are expected to remain transparent throughout the remainder of the visible region. Furthermore, the molar absorptivity increases with the number of fixed-length linearly conjugated paths. This is in significant contrast to the behaviour of linearly conjugated polydiacetylenes that show large increases of λ_{max} with similar chain length extension, while maintaining a relatively constant molar absorptivity at λ_{max} [25, 26].

These results show that electronic characteristics of the iso-PDAs are dominated primarily by contributions from the longest linearly conjugated segment present in the molecules (shown in bold in for the dimer and the heptamer in figure 3),

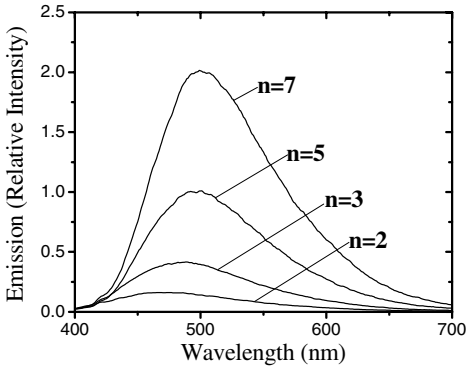

Figure 5. Electronic emission spectra for iso-PDAs, as measured in $CHCl_3$.

while contributions from cross conjugation are minimal or absent.

Unlike the absorption energies for these four compounds, the photoluminescence emission energy is more dependent on oligomer length. Figure 5 shows the emission spectra for the iso-PDAs. The emission wavelength of the heptamer is red-shifted by about 25 nm in comparison to that of the dimer. The similar emission wavelength for the pentamer and heptamer, however, suggests that saturation has already been reached.

Table 1 lists the molecular hyperpolarizabilities for each of the oligomers, as well as the nonlinearity relative to THF. Figure 6 shows the concentration-normalized DOKE signals for the oligomer series, with each time-resolved plot the result of five averaged scans. The molecular second hyperpolarizabilities were obtained from the peak signals in figure 6, using

$$\gamma_S = \frac{\chi_R^{(3)}(\phi_S/\phi_R - 1)}{L^4 N_C}. \tag{6}$$

The requisite $\chi^{(3)}$ values were obtained from the following relationship:

$$\chi_S^{(3)} = \chi_R^{(3)}\left(\frac{\phi_S}{\phi_R}\right), \tag{7}$$

where $\chi_S^{(3)}$ and $\chi_R^{(3)}$ are, respectively, the sample and reference susceptibilities and ϕ_S and ϕ_R are, respectively, the measured rotation in polarization of the sample and reference.

THF was used as a reference for all samples. Using the treatment described above, we obtain a reference value of $\chi_R^{(3)} = 2.1 \times 10^{-14}$ esu. It should be noted that $\chi_R^{(3)}$ is not $\chi_{THF}^{(3)}$, as it includes contributions of the quartz cuvette[4]. Separating the effects of the sample holder yields[5] $\chi_{THF}^{(3)} = (1.2 \pm 0.3) \times 10^{-14}$ esu and $\gamma_{THF} = (5.2 \pm 1.3) \times 10^{-37}$ esu, which compare reasonably well with reported values of $\chi_{THF}^{(3)} = 3.7 \times 10^{-14}$ esu ($\lambda = 620$ nm) [27] and $\gamma_{THF} = 4.8 \times 10^{-37}$ esu [28]. Maximum signals are observed at zero probe delay times, suggesting that the ultrafast electronic response is the dominant contributor to the observed nonlinearities.

[4] A full discussion of signal analysis and blank separation is beyond the scope of this paper. Briefly, $\chi_R^{(3)}$ and γ_R refer to signals that include the sample holders, whereas $\chi_{THF}^{(3)}$ and γ_{THF} refer to pure THF values.

[5] Uncertainty in these values comes from uncertainties in pulse-shape/power diagnostics as well as signal analysis. The error in γ reported is due to uncertainties in signal analysis alone, as a precise $\chi^{(3)}$ is assumed.

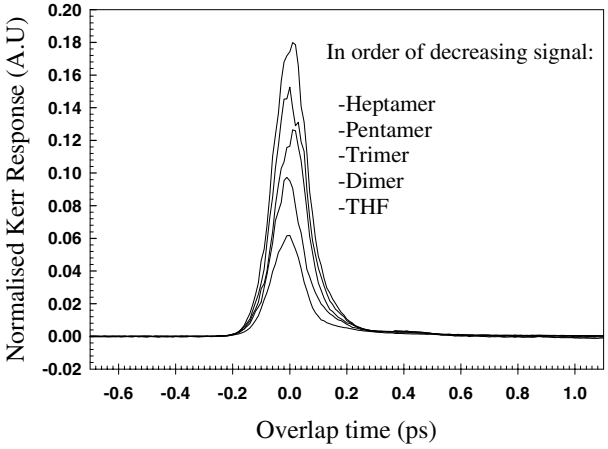

Figure 6. Time resolved Kerr response for iso-PDAs relative to THF reference. Signals have been concentration normalized.

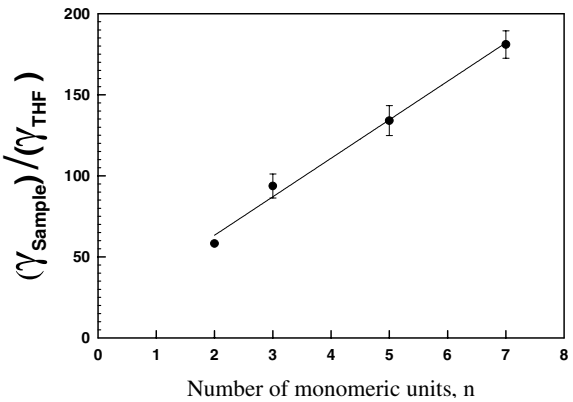

Figure 7. Sample hyperpolarizability, γ, relative to absolute THF hyperpolarizability, with a regression line, displaying linear hyperpolarizability-to-chain-length behaviour.

The relative γ values in table 1 are displayed in figure 7 and show that the molecular hyperpolarizabilities increase as a function of oligomer length. This increase, however, is proportional to the number of linearly conjugated segments within each molecule in the progression from dimer to heptamer. As a result, the optical nonlinearities of these samples appear to be governed by polarization along the linearly conjugated paths, with little or no additional contribution from cross conjugation.

4. Conclusions

The linear and third-order NLO properties of cross-conjugated, iso-PDAs have been explored as a function of oligomer length. These compounds show a linear increase in molecular second hyperpolarizability, γ, as the chain length is increased from the dimer to the heptamer. This increase in γ can be attributed to an increase in the number of fixed-length linearly conjugated paths. No added contribution to the nonlinear response attributable to the cross-conjugated backbone has been observed. Extension of this study to include longer oligomers is under way, and should provide more concrete trends in sample nonlinearities.

Acknowledgments

This research was supported by NSERC, CFI, IIPP, ASRA, CIPI, iCORE and PetroCanada (Young Innovator Award to RRT).

References

[1] Stegeman G I and Miller A 1993 *Photonics in Switching: 1. Background and Component* ed J E Midwinter (Boston, MA: Academic)
[2] Brédas J-L, Adant C, Tackx P and Persoons A 1994 *Chem. Rev.* **94** 243
[3] Prasad P N and Williams D J 1991 *Introduction to Nonlinear Optical Effects in Molecules and Polymers* (New York: Wiley–Interscience)
[4] Tykwinski R R, Gubler U, Martin R E, Diederich F, Bosshard C and Günter P 1998 *J. Phys. Chem.* B **102** 4451
[5] Nalwa H S 1997 *Nonlinear Optics of Organic Molecules and Polymer* ed H S Nalwa and S Miyata (New York: Chemical Rubber Company Press) pp 571–797
[6] Bubeck C 1998 *Electronic Materials: The Oligomer Approach* ed K Mullen and G Wegner (Chichester: Wiley–VCH)
[7] Kuzyk M G and Dirk C W (ed) 1998 *Characterization Techniques and Tabulations for Organic Nonlinear Optical Materials* (New York: Dekker)
[8] Agrawal G P, Cojan C and Flytzanis C 1978 *Phys. Rev.* B **17** 776
[9] Samuel I D W, Ledoux I, Dhenaut J, Zyss J, Fox H H, Schrock R R and Silbey R J 1994 *Science* **265** 1070
[10] Tretiak S, Chernyak V and Mukamel S 1996 *Phys. Rev. Lett.* **77** 4656
[11] Moylan C R, Twieg R J, Lee V Y, Swanson S A, Betterton K M and Miller R D 1993 *J. Am. Chem. Soc.* **115** 12 599
[12] Blanchard-Desce M, Baudin J B, Jullien L, Lorne R, Ruel O, Brasselet S and Zyss J 1999 *Opt. Mater.* **12** 333
[13] Ledoux I, Zyss J, Jutand A and Amatore C 1991 *Chem. Phys.* **150** 117
[14] Slepkov A D, Hegmann F A, Zhao Y, Tykwinski R R and Kamada K 2002 *J. Chem. Phys.* **116** 3834
[15] Wu Q, Lit M and Zhang X-C 1996 *Appl. Phys. Lett.* **68** 2924
[16] Lui K P H and Hegmann F A 2001 *Appl. Phys. Lett.* **78** 3478
[17] Ho A A and Alfano R R 1979 *Phys. Rev.* A **20** 2170
[18] Ho A A 1984 *Semiconductors Probed by Ultrafast Laser Spectroscopy* vol 2, ed R R Alfano (New York: Academic) pp 409–39
[19] Kuzyk M G, Norwood R A, Wu J W and Garito A F 1989 *J. Opt. Soc. Am.* B **6** 154
[20] Pang Y, Samoc M and Prasad P N 1991 *J. Chem. Phys.* **94** 5282
[21] Butcher P N and Cotter D 1990 *The Elements of Nonlinear Optics* (Cambridge: Cambridge University Press)
[22] Scarparo M A F, Song J J, Lee J H, Cromer C and Levenson M D 1979 *Appl. Phys. Lett.* **35** 490
[23] Kamada K, Ueda M, Sakaguchi T, Ohta K and Fukumi T 1998 *J. Opt. Soc. Am.* B **15** 838
[24] Zhao Y and Tykwinski R R 2002 unpublished
[25] Giesa R, Klapper M and Schultz R C 1991 *Makromol. Chem., Makromol. Symp.* **44** 1
[26] Byrne H J, Blau W, Giesa R and Schulz R C 1990 *Chem. Phys. Lett.* **167** 484
[27] Orczyk M E, Samoc M, Swiatkiewicz J and Prasad P N 1993 *J. Chem. Phys.* **98** 2524
[28] Porter P L, Guha S, Kang K and Frazier C C 1991 *Polymer* **32** 1756